An adjoint variable method for the topological derivative of the tangent derivative of boundary data

Peijun TANG[1)], Kei MATSUSHIMA[2)], Hiroshi ISAKARI[3)], Toru TAKAHASHI[4)], Toshiro MATSUMOTO[5)]

1) Nagoya University (Furo-cho, Chikusa-ku, Nagoya, Aichi, 464-8603, E-mail: tangpeijun@nuem.nagoya-u.ac.jp)
2) Nagoya University (Furo-cho, Chikusa-ku, Nagoya, Aichi, 464-8603, E-mail: k_matusima@nuem.nagoya-u.ac.jp)
3) Nagoya University (Furo-cho, Chikusa-ku, Nagoya, Aichi, 464-8603, E-mail: isa@nagoya-u.jp)
4) Nagoya University (Furo-cho, Chikusa-ku, Nagoya, Aichi, 464-8603, E-mail: ttaka@nuem.nagoya-u.ac.jp)
5) Nagoya University (Furo-cho, Chikusa-ku, Nagoya, Aichi, 464-8603, E-mail: t.matsumoto@nuem.nagoya-u.ac.jp)

This paper discusses the topological derivative for objective functionals associated with the tangent derivatives of physical quantities such as strains and stresses on the boundary of an elastic domain. We first show that it is necessary to adopt adjoint variables defined in the sense of generalised function to construct the adjoint variable method for such a topological derivative. We also show that the newly defined adjoint "variable" can easily be computed by the boundary element method. We then implement a topology optimisation algorithm based on the level-set method using the derived topological derivative. The effectiveness of the proposed method is demonstrated by addressing a defect identification problem using the measured tangent component of the strain on the boundary.

Key Words: Topology optimization, Topological derivative, Level-set method, Inverse problem, Shape functional related to strain and/or stress, Adjoint variable method

1. Introduction

With the long-foot development of computational mechanics and the extensive application of computer-aided engineering (CAE) in many manufacturing departments, computer simulation has no longer limited itself to performance evaluation but extended to the design process for modern manufacturers. Among simulation-based design methods, the topology optimisation might be the most versatile one equipped with the freedom to generate change not only on the outer shape but also on the topology during the optimisation process. For obtaining optimal results, the topology optimisation is firstly introduced by Bendsøe and Kikuchi[(1)], which is built based on homogenisation. After that, the density method is proposed by Bendsøe[(2)]. Due to the regularisation necessary in both the methods, they may suffer from so called grayscale problem. The optimised structure by the homogenisation and density methods may include the part between structure and cavity. To resolve the issue, another type of the topology optimisation using the shape representation by the level-set method is introduced. The level-set method implicitly expresses the target structural configurations by the iso-surface of a scalar function. So far, several level-set-based topology optimisation are proposed[(3, 4, 5, 6)]. Now, all the types of the topology optimisations mentioned above are widely accepted and applied to various design problems mainly in structural mechanics.

Most literature on topology optimisation are concerning the topics of compliance and frequency response, which partially neglected actual working conditions on products. Design with high stiffness may result in low durability if stress is not taken into account[(7)]. Thus, some authors have proposed topology optimisations concerning stress distribution. For example, Le et al[(8)] proposed an effective algorithm to resolve the stress-constrained topology optimisation. Bruggi et al[(9)] presented a method designing elastic structures with minimum weight subject to compliance and local stress constraints. Delgado and Bonnet[(10)] derived the topological derivative for stress-based shape functional.

All of the publications mentioned here deal with stresses defined in a region as the objective functional. To the best of the authors' knowledge, the topology optimisation concerning the boundary stress has not yet been proposed. Since stress concentrations often occur in the vicinity of boundaries, it may be worthwhile to construct a topology optimisation that can control the stresses on the boundary. Also, since strain is a quantity usually measured on the boundary using a strain gauge, it may also be of value for topology optimisation to control boundary strain. It is, however, difficult to compute the topological derivative of objective function defined in terms of boundary stresses and strains using the usual adjoint variable method. The essential diffi-

Received Nov. 4, 2020, accepted Nov. 20, 2020

culty stems from the fact that any standard adjoint variable cannot cancel out the variation of the tangent derivative of the boundary displacement due to the topological change.

In this study, we show that, by using an adjoint variable defined as a generalised function, we can compute the topological derivative for the tangent derivative of a physical quantity defined on a boundary. We incorporate the derived topological derivatives into a topology optimisation scheme based on the level-set method[6] and the boundary element method (BEM). We demonstrate the effectiveness of the proposed method by solving an inverse problem to find cavities from the measured strain data on the boundary.

2. Linear elastodynamics and BEM

In this section, we present basic equations for an elastodynamic problem in two dimensions which serves as a constraint for our topology optimisation. We also present a BEM for the elastodynamics.

2.1. Fundamental equations

We here consider a bounded region $\Omega \subset \mathbb{R}^2$ filled with an isotropic linear elastic material oscillating harmonically with the angular frequency ω. The oscillation in Ω is governed by the following boundary value problem:

$$C_{ijkl} u_{k,lj}(\boldsymbol{x}) + \rho\omega^2 u_i(\boldsymbol{x}) = 0 \quad \boldsymbol{x} \in \Omega, \tag{1}$$

$$u_i(\boldsymbol{x}) = \bar{u}_i(\boldsymbol{x}) \quad \boldsymbol{x} \in \Gamma_u \subset \Gamma := \partial\Omega, \tag{2}$$

$$t_i(\boldsymbol{x}) = \bar{t}_i(\boldsymbol{x}) \quad \boldsymbol{x} \in \Gamma_t = \Gamma \setminus \Gamma_u, \tag{3}$$

where $\boldsymbol{u}$ represents the complex amplitude of the displacement with which its time domain counterpart is recovered as $\Re[\boldsymbol{u}(\boldsymbol{x})e^{-\mathrm{i}\omega t}]$. $t_i = \sigma_{ji} n_j$ is the traction, and $\boldsymbol{\sigma}$ is the stress, $\boldsymbol{n}$ is the unit normal vector on Γ directed from Ω. The prescribed displacement $\bar{\boldsymbol{u}}$ and traction $\bar{\boldsymbol{t}}$ are given on Γ_u and Γ_t, respectively. Assuming the plane-strain state, $C_{ijkl} = \lambda\delta_{ij}\delta_{kl} + \mu(\delta_{ik}\delta_{jl} + \delta_{ul}\delta_{jk})$ represents the elastic tensor which relates the stress with the strain as $\sigma_{ij} = C_{ijkl}\varepsilon_{kl}$, λ and μ are the Lamé constants, δ_{ij} is Kronecker's delta, and ρ denotes the density of the material. With the assumption of small deformation, the strain $\boldsymbol{\varepsilon}$ admits the following expression:

$$\varepsilon_{ij} = \frac{1}{2}\left(u_{i,j} + u_{j,i}\right). \tag{4}$$

2.2. Boundary element method

The integral representation of the solution in Ω for the boundary value problem (1)–(3) is given as follows:

$$u_i(\boldsymbol{x}) = [\mathcal{U}_\Gamma \boldsymbol{t}]_i(\boldsymbol{x}) - [\mathcal{T}_\Gamma \boldsymbol{u}]_i(\boldsymbol{x}), \tag{5}$$

where the operators $\mathcal{U}$ and $\mathcal{T}$ are respectively given as follows:

$$[\mathcal{U}_\Gamma \boldsymbol{t}]_i(\boldsymbol{x}) = \int_\Gamma U_{ij}(\boldsymbol{x}-\boldsymbol{y}) t_j(\boldsymbol{y}) d\Gamma(\boldsymbol{y}) \tag{6}$$

$$[\mathcal{T}_\Gamma \boldsymbol{u}]_i(\boldsymbol{x}) = \int_\Gamma T_{ij}(\boldsymbol{x}-\boldsymbol{y}) u_j(\boldsymbol{y}) d\Gamma(\boldsymbol{y}) \tag{7}$$

where U_{ij} and T_{ij} are the fundamental solution for 2D elastodynamics and the kernel of double layer, respectively. The unknown quantities in (5), i.e. $\boldsymbol{u}$ on Γ_t, and $\boldsymbol{t}$ on Γ_u can be found by solving the following boundary integral equation:

$$c_{ij}(\boldsymbol{x}) u_j(\boldsymbol{x}) = [\mathcal{U}_\Gamma \boldsymbol{t}]_i(\boldsymbol{x}) - [\mathcal{T}_\Gamma \boldsymbol{u}]_i(\boldsymbol{x}), \tag{8}$$

for $\boldsymbol{x} \in \Gamma$, where the coefficient in the left-hand side is $c_{ij}(\boldsymbol{x}) = \delta_{ij}/2$ if Γ is smooth around $\boldsymbol{x}$. On the discretisation for (8), we here use the collocation with quadratic elements.

Other than the displacement on Γ and in Ω, we can obtain the strain and stress by BEM. For an interior point $\boldsymbol{x} \in \Omega$, they can be computed via the gradient of the integral representation (5), the definition of the strain (4), and so forth. For the boundary data, both the strain and stress can be expressed by the traction and tangent derivative of the displacement as

$$\begin{aligned}\varepsilon_{ij} = {} & \frac{1}{2}\left(\frac{\partial u_i}{\partial \boldsymbol{s}} s_j + \frac{\partial u_j}{\partial \boldsymbol{s}} s_i\right) \\ & + \frac{n_j}{2}\left[\frac{1}{\mu}\left(\delta_{il} - \frac{\lambda+\mu}{\lambda+2\mu} n_i n_l\right) t_l - \left(\frac{\lambda}{\lambda+\mu} n_i s_l + n_l s_i\right)\frac{\partial u_l}{\partial \boldsymbol{s}}\right] \\ & + \frac{n_i}{2}\left[\frac{1}{\mu}\left(\delta_{jl} - \frac{\lambda+\mu}{\lambda+2\mu} n_j n_l\right) t_l - \left(\frac{\lambda}{\lambda+\mu} n_j s_l + n_l s_j\right)\frac{\partial u_l}{\partial \boldsymbol{s}}\right],\end{aligned} \tag{9}$$

$$\sigma_{kl} = \alpha_{kli} t_i + \beta_{kli} \frac{\partial u_i}{\partial \boldsymbol{s}}, \tag{10}$$

where the coefficients α_{kli} and β_{kli} are given as

$$\alpha_{kli} = \frac{1}{\lambda+2\mu}\left[\lambda\delta_{kl} - 2(\lambda+\mu) n_k n_l\right] n_i + \left(\delta_{ki} n_l + \delta_{li} n_k\right), \tag{11}$$

$$\begin{aligned}\beta_{kli} = {} & \frac{2\lambda\mu}{\lambda+2\mu}\left(\delta_{kl} - n_k n_l\right) s_i \\ & + \mu\left(\delta_{ki} - n_k n_i\right) s_l + \mu\left(\delta_{li} - n_l n_i\right) s_k,\end{aligned} \tag{12}$$

and $\partial/\partial\boldsymbol{s}$ represents the operator for the tangent derivative, and $\boldsymbol{s} = (s_1, s_2)^t$ is the unit tangent vector satisfying $(s_1, s_2, 0)^t = (0,0,1)^t \times (n_1, n_2, 0)^t$. Since the traction is obtained by solving the boundary integral equation (8), one additional task to obtain boundary strain and stress is to evaluate the tangent derivative of the displacement $\partial\boldsymbol{u}/\partial\boldsymbol{s}$ which can be computed by differentiating the basis function for $\boldsymbol{u}$. For simplicity, we henceforth denote $\partial\boldsymbol{u}/\partial\boldsymbol{s}$ as $\boldsymbol{u}'$.

3. Topology optimisation

In this section, we present a topology optimisation related to the shape functional written in terms of stress and strain on the boundary of an elastic material.

3.1. Objective function

Our objective is to find an optimal distribution of elastic region $\Omega \subset D$, under the constrain condition (1)–(3), minimising the following shape functional associated with strain and/or stress:

$$J(\Omega) = \int_{\Gamma_f} F(\boldsymbol{\varepsilon}, \boldsymbol{\sigma}) d\Gamma, \tag{13}$$

where F is a functional, D is a preset design domain, and Γ_f is a part of Γ i.e $\Gamma_f \subset \Gamma$. According to the discussion

in the previous section, the objective functional (13) can be rewritten as

$$J = \int_{\Gamma_f} f(\boldsymbol{u}', \boldsymbol{t}) d\Gamma, \tag{14}$$

in terms of the traction and tangent derivative of the displacement, where f is a functional.

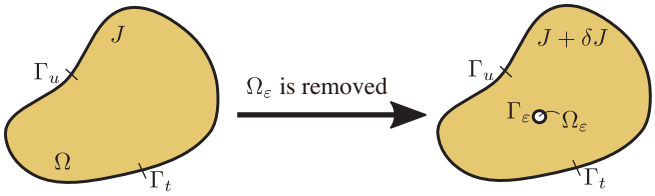

Fig. 1 Topological change in Ω. An infinitesimal cavity Ω_ε introduced at $\boldsymbol{x}^0$ causes the change in the objective function as $J \to J + \delta J(\boldsymbol{x}^0)$ along with the changes in physical quantities such as displacement, traction, strain, and stress.

3.2. Topological derivative

One of the key ingredients for establishing a topology optimisation for (14) is the topological derivative. In this section, we derive the topological derivative for (14) with the help of the adjoint variable method. As shown in Fig. 1, let us assume that an infinitesimal circular cavity Ω_ε (whose radius and centre are ε and $\boldsymbol{x}^0$, respectively) is generated in Ω, and the physical quantities change accordingly as, for example, $\boldsymbol{u} \to \boldsymbol{u} + \delta\boldsymbol{u}$. We here assume that the boundary condition on $\Gamma_\varepsilon := \partial\Omega_\varepsilon$ is traction free. Due to the linearity of the problem, a governing equation for the perturbations can be obtained as

$$C_{ijkl}\delta u_{k,lj}(\boldsymbol{x}) + \rho\omega^2 \delta u_i(\boldsymbol{x}) = 0 \qquad \boldsymbol{x} \in \Omega \setminus \overline{\Omega_\varepsilon}, \tag{15}$$

$$\delta u_i(\boldsymbol{x}) = 0 \qquad \boldsymbol{x} \in \Gamma_u, \tag{16}$$

$$\delta t_i(\boldsymbol{x}) = 0 \qquad \boldsymbol{x} \in \Gamma_t, \tag{17}$$

$$\delta t_i(\boldsymbol{x}) = -t_i(\boldsymbol{x}) \qquad \boldsymbol{x} \in \Gamma_\varepsilon, \tag{18}$$

where the unit normal vector on Γ_ε is defined positive when directed from $\Omega \setminus \overline{\Omega_\varepsilon}$.

The objective function also changes accordingly as $J \to J + \delta J(\boldsymbol{x}^0)$. The perturbation in J is given as

$$\delta J(\boldsymbol{x}^0) = \Re\left[\int_{\Gamma_t} \frac{\partial f}{\partial u_i'} \delta u_i' d\Gamma + \int_{\Gamma_u} \frac{\partial f}{\partial t_i} \delta t_i d\Gamma\right]. \tag{19}$$

Note that, to derive (19), we used the boundary conditions (16) and (17). To evaluate (19), we introduce the adjoint displacement $\tilde{\boldsymbol{u}}$ satisfying the following Navier's equation:

$$C_{ijkl}\tilde{u}_{k,lj}(\boldsymbol{x}) + \rho\omega^2 \tilde{u}_i(\boldsymbol{x}) = 0 \qquad \boldsymbol{x} \in \Omega. \tag{20}$$

Betti's reciprocity theorem for δu_i and $\tilde{u}_i$ in $\Omega \setminus \overline{\Omega_\varepsilon}$ gives the following identity:

$$\int_{\Gamma \cup \Gamma_\varepsilon} \left(\tilde{t}_i \delta u_i - \tilde{u}_i \delta t_i\right) d\Gamma = 0, \tag{21}$$

in which $\tilde{\boldsymbol{t}}$ is the adjoint traction on the boundary $\Gamma \cup \Gamma_\varepsilon$ corresponding to $\tilde{\boldsymbol{u}}$ defined as

$$\tilde{t}_i(\boldsymbol{x}) = C_{ijkl}\tilde{u}_{k,l}(\boldsymbol{x}) n_j(\boldsymbol{x}). \tag{22}$$

By using the boundary conditions (16)$\sim$(18), we can rewrite (21) as follows:

$$\begin{aligned} 0 &= \int_{\Gamma \cup \Gamma_\varepsilon} \left(\tilde{t}_i \delta u_i - \tilde{u}_i \delta t_i\right) d\Gamma \\ &= -\int_{\Gamma_u} \tilde{u}_i \delta t_i d\Gamma + \int_{\Gamma_t} \tilde{t}_i \delta u_i d\Gamma + \int_{\Gamma_\varepsilon} \left(\tilde{t}_i \delta u_i + \tilde{u}_i t_i\right) d\Gamma \end{aligned} \tag{23}$$

As usual, by subtracting the real part of (23) from (19), one has

$$\begin{aligned} \delta J(\boldsymbol{x}^0) = \Re\Bigg[&\int_{\Gamma_u} \left(\frac{\partial f}{\partial t_i} + \tilde{u}_i\right) \delta t_i d\Gamma \\ &+ \int_{\Gamma_t} \left(\frac{\partial f}{\partial u_i'} \delta u_i' - \tilde{t}_i \delta u_i\right) d\Gamma \\ &- \int_{\Gamma_\varepsilon} \left(\tilde{t}_i \delta u_i + \tilde{u}_i t_i\right) d\Gamma\Bigg]. \end{aligned} \tag{24}$$

If one can impose the boundary conditions for the adjoint quantities (with tilde) so that the first and second terms in (24) vanish for arbitrary perturbations (with δ), δJ is expressed only by the quantities defined on Γ_ε whose asymptotic behaviours in $\varepsilon \downarrow 0$ are tractable.

To define such an adjoint system, we first introduce a generalised function $\psi\mathcal{S}$ which satisfies

$$\int_{\Gamma_t} \varphi(\boldsymbol{x})[\psi\mathcal{S}](\boldsymbol{x}) d\Gamma(\boldsymbol{x}) = \int_{\Gamma_t} \frac{\partial \varphi}{\partial \boldsymbol{s}}(\boldsymbol{x}) \psi(\boldsymbol{x}) d\Gamma(\boldsymbol{x}) \tag{25}$$

for an arbitrary function φ and a given function ψ. We then define the adjoint system by the following integral representation

$$\tilde{u}_i(\boldsymbol{x}) = \left[\mathcal{U}_{\Gamma_t}' \frac{\partial f}{\partial \boldsymbol{u}'}\right]_i + \left[\mathcal{U}_{\Gamma_u} \tilde{\boldsymbol{t}}\right]_i + \left[\mathcal{T}_{\Gamma_u} \frac{\partial f}{\partial \boldsymbol{t}}\right]_i - \left[\mathcal{T}_{\Gamma_t} \tilde{\boldsymbol{u}}\right]_i \tag{26}$$

for $\boldsymbol{x} \in \Omega$, with $\tilde{\boldsymbol{u}}$ and $\tilde{\boldsymbol{t}}$ solving the following integral equation (for $\boldsymbol{x} \in \Gamma$):

$$c_{ij}\tilde{u}_j + \left[\mathcal{T}_{\Gamma_t} \tilde{\boldsymbol{u}}\right]_i - \left[\mathcal{U}_{\Gamma_u} \tilde{\boldsymbol{t}}\right]_i = \left[\mathcal{U}_{\Gamma_t}' \frac{\partial f}{\partial \boldsymbol{u}'}\right]_i + \left[\mathcal{T}_{\Gamma_u} \frac{\partial f}{\partial \boldsymbol{t}}\right]_i, \tag{27}$$

where the integral operator $\mathcal{U}'$ is defined as

$$\left[\mathcal{U}_\Gamma' \frac{\partial f}{\partial \boldsymbol{u}'}\right]_i (\boldsymbol{x}) = \int_\Gamma \frac{\partial U_{ij}}{\partial \boldsymbol{s}}(\boldsymbol{x} - \boldsymbol{y}) \frac{\partial f}{\partial u_j'}(\boldsymbol{y}) d\Gamma(\boldsymbol{y}). \tag{28}$$

The boundary value problem corresponding to (27) can formally be given as

$$C_{ijkl}\tilde{u}_{k,lj}(\boldsymbol{x}) + \rho\omega^2 \tilde{u}_i(\boldsymbol{x}) = 0 \qquad \boldsymbol{x} \in \Omega, \tag{29}$$

$$\tilde{u}_i(\boldsymbol{x}) = -\frac{\partial f}{\partial t_i}(\boldsymbol{x}) \qquad \boldsymbol{x} \in \Gamma_u, \tag{30}$$

$$\tilde{t}_i(\boldsymbol{x}) = \left[\frac{\partial f}{\partial u_i'} \mathcal{S}\right](\boldsymbol{x}) \qquad \boldsymbol{x} \in \Gamma_t. \tag{31}$$

where in this case $\mathcal{S}$ is the tangential differential operator, i.e., $\mathcal{S} = \partial/\partial s$. In this sense, we temporary call Eqs.(29)$\sim$(31) here a *boundary operator problem*.

With the adjoint "variables" $\tilde{\boldsymbol{u}}$ and $\tilde{\boldsymbol{t}}$ defined above, (24) is reduced to

$$\delta J(\boldsymbol{x}^0) = \Re\left[-\int_{\Gamma_\varepsilon} (\bar{t}_i \delta u_i + \tilde{u}_i t_i) d\Gamma\right]. \tag{32}$$

The remaining task to obtain the topological derivative is to check the asymptotic behaviour as $\varepsilon \downarrow 0$ of the quantities in the integrand in (32). For this standard procedure, see our previous publication[11] for example. The final expression for the topological derivative

$$\mathcal{D}_{\mathrm{T}} J(\boldsymbol{x}^0) = \lim_{\epsilon \downarrow 0} \frac{\delta J(\boldsymbol{x}^0)}{\pi \varepsilon^2}, \tag{33}$$

is obtained as

$$\mathcal{D}_{\mathrm{T}} J(\boldsymbol{x}) = \mathrm{Re}\left[\frac{\lambda + 2\mu}{4\mu\,(\lambda + \mu)} \left(4\sigma_{ij}(\boldsymbol{x})\tilde{\sigma}_{ij}(\boldsymbol{x}) - \sigma_{ii}(\boldsymbol{x})\tilde{\sigma}_{jj}(\boldsymbol{x})\right) - \rho\omega^2 u_i(\boldsymbol{x})\tilde{u}_i(\boldsymbol{x})\right], \tag{34}$$

where $\tilde{\boldsymbol{\sigma}}$ is the stress associated with $\tilde{\boldsymbol{u}}$. Equation (34) has been derived by starting from the expression of the variation of the objective functional of Eq.(32). Therefore, the adjoint problem is appropriately defined so that δJ take the expression of Eq.(32), the topological derivative can always be calculated using Eq.(34).

Note that, to compute the layer potential (28), we need to deal with the strong singular integral which cannot be evaluated by the technique used for the second layer potential (7) involving the rigid body motion. Instead, we here adopt the method proposed by Guiggiani and Casalini[12] which directly computes the singular integral (28) in the Cauchy principle sense.

3.3. Level-set method

With the topological derivative derived in the previous section, the optimisation problem minimising (14) subject to (1)∼(3) is solved by a level-set-based optimiser[6], which assumes that the level set function $\phi(\boldsymbol{x})$, defined as $0 < \phi(\boldsymbol{x}) \leq 1$ for $\boldsymbol{x} \in \Omega$, $\phi(\boldsymbol{x}) = 0$ for $\boldsymbol{x} \in \Gamma$, and $-1 \leq \phi(\boldsymbol{x}) < 0$ for $\boldsymbol{x} \in D \setminus \Omega$. The material domain can be extracted from the distribution of $\phi(\boldsymbol{x})$, and its evolution is assumed to follow

$$\frac{\partial \phi}{\partial t} = K\left(\mathcal{D}_{\mathrm{T}} + \tau \nabla^2 \phi\right) \tag{35}$$

Equation (35) is solved by FEM easily for a fixed domain D utilizing the values of $\mathcal{D}_{\mathrm{T}}$ iteratively, causing the change in the distribution of $\phi(\boldsymbol{x})$.

4. Numerical examples

In this section, we check the validity of the proposed topology optimisation. To this end, we solve inverse scattering problems (Fig. 2) to find preset defects inside the square region D by minimising the following shape functional

$$J = \sum_{i=1}^{4} \int_{\Gamma_i} f_i(\boldsymbol{\varepsilon}) d\Gamma, \tag{36}$$

where f_i is defined in Fig. 2, and $\boldsymbol{\varepsilon}^{\mathrm{m}}$ is the measured data for the strain. Thus, we explore the shape of defects by

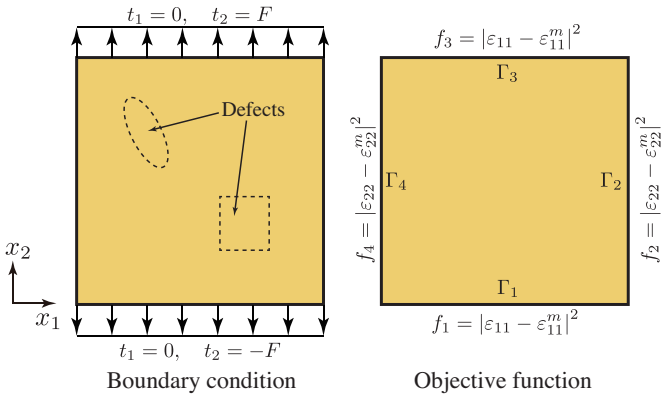

Fig. 2 Settings for the inverse scattering. The left shows the boundary condition, and the right shows the definition of the objective function.

minimising the misfit in the tangent components of strain for the trial defect ($\boldsymbol{\varepsilon}$) and target one ($\boldsymbol{\varepsilon}^{\mathrm{m}}$). Note that, in all the examples in this section, the measurement data is obtained by BEM. We chose the inverse scattering problem with which the "optimal" shape is available rather than the standard topology optimisation problem because it is useful to assess the performance of the proposed method.

In all the examples to follow, the area size of the design domain is 1.0×1.0 which is divided into 40×40 finite elements on which the level-set function is expanded[6]. The uniformly distributed excitation is given as $\bar{t}_1 = 0$, $\bar{t}_2 = F = 0.1 \times 10^{10}$ and $\bar{t}_1 = 0$, $\bar{t}_2 = -F$ on upper (Γ_3) and lower (Γ_1) sides of the domain with excitation angular frequency of $\omega = 500$ [rad/s], respectively. The rest of the boundary is traction-free. Material parameters are given as $E = 2.16 \times 10^{10}$ [Pa], $\nu = 0.30$ and $\rho = 7850$ [kg/m^3]. Also, the parameters of Eq.(35) are set as $K = 1$ and $\tau = 4 \sim 5$. Fig. 3.

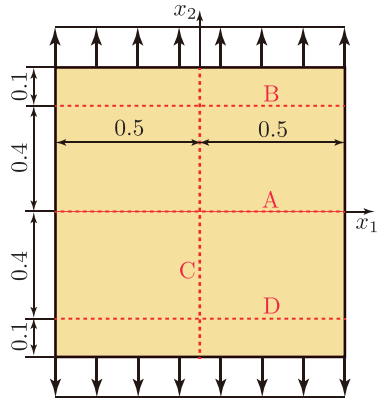

Fig. 3 Verification of topological derivative.

4.1. Circular cavity

Let us first consider a circular cavity of radius 0.2 centred at the square region D as the target.

With this setting, we first check the correctness of the

topological derivative (34). To this end, we compute (34) as well as its finite-difference approximation with $\varepsilon = 0.01$ on the lines A, B, C, and D in In Fig. 4∼Fig. 7, the red crosses and green lines show the topological derivative computed by the present adjoint formulation and the finite-difference approximation, respectively. As the figures show, the present approach can accurately compute the topological derivative of a shape functional related to tangent derivative of the displacement.

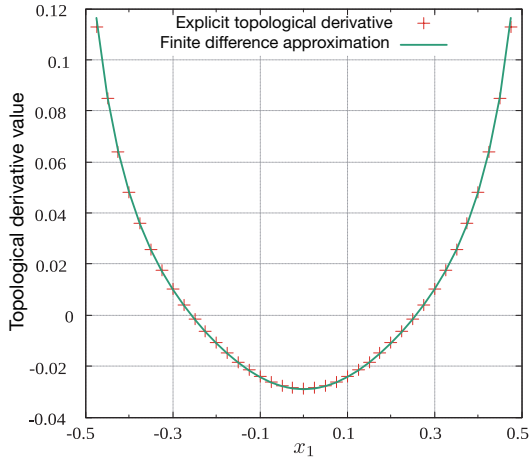

Fig. 4 Topological derivatives along the line A.

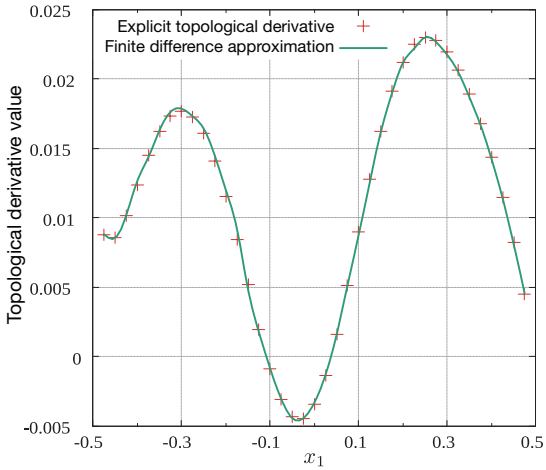

Fig. 5 Topological derivatives along the line B.

We then show the numerical result for the inverse scattering. From the square region D filled with the elastic material, we explored the target shape with the circular cavity by minimising the objective function (36). The history of the estimated shape and the convergence curve of the objective functional are respectively given in Fig. 8 and Fig. 9. Although the obtained cavity shapes are a little bit wavy, they may become more smoother for larger value of the regularisation parameter τ.

As shown in Fig. 8, a cavity created at step 9 gradually

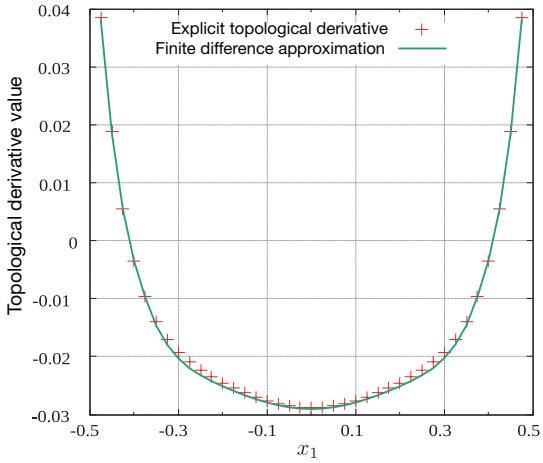

Fig. 6 Topological derivatives along the line C.

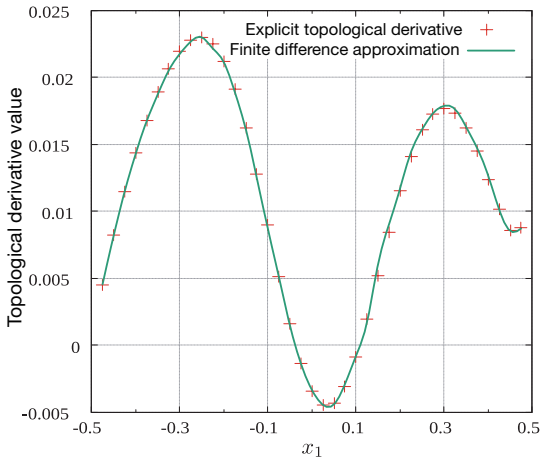

Fig. 7 Topological derivatives along the line D.

becomes large and almost coincides with the target circular cavity at step 27 after which the shape is not improved anymore. This can also be confirmed by the convergence curve in Eq.(9). A small increase in the objective functional value at step 18 was caused by the appearance of some projections of the cavity shape, but after they disappeared, the objective functional value decreased promptly.

4.2. Cavities of various shapes

We have also tested the proposed method with cavities in various shape such as square, triangle, and oval. Other than the target shape, all the settings are exactly the same as the ones in the previous examples. We show the optimised shapes in Fig. 10

Also, the initial and optimised objective values for all the cases are listed in Table 1.

From Fig. 10 and Table 1, we conclude that the proposed method can find a cavity from the measured boundary strain data regardless of its shape, which which we conclude that the present topological derivative works well to minimise the objective function related to the tangent derivative of bound-

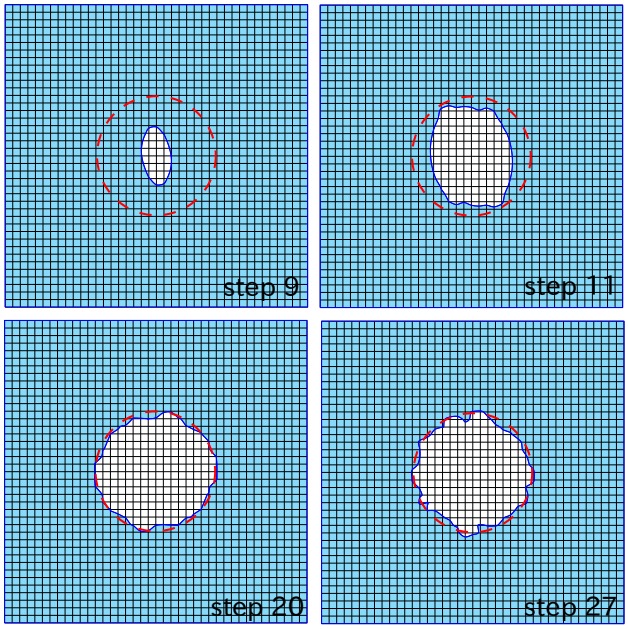

Fig. 8 History of the estimated defect configuration for the circular case. The red dashed line shows the boundary of the target defect.

ary quantities.

Table 1: Initial and optimised objective values for inverse problems with various cavities.

Cavity	J_{init}	J_{opt}
Square	0.148550×10^{-3}	0.412530×10^{-7}
Triangle	0.151078×10^{-2}	0.822205×10^{-6}
Oval	0.615921×10^{-3}	0.547446×10^{-6}

5. Conclusion

In this paper, we proposed a new adjoint field to evaluate the topological derivative of the tangent derivative of displacement. We showed that the newly derived topological derivative can easily be evaluated by BEM. We also implemented a topology optimiser using the level-set method to optimise the boundary strain. With several examples related to inverse scattering problems, we conclude that the proposed method can find an optimal design minimising the objective function defined in terms of boundary strain. Future investigation may include more rigorous mathematical justification for the newly defined adjoint variable, and extend the proposed method to optimise boundary stress.

Acknowlegement

This work was partially supported by the Grant-in-Aid for Scientific Research (A), No.19H00740, of the Japan Society for the Promotion of Science.

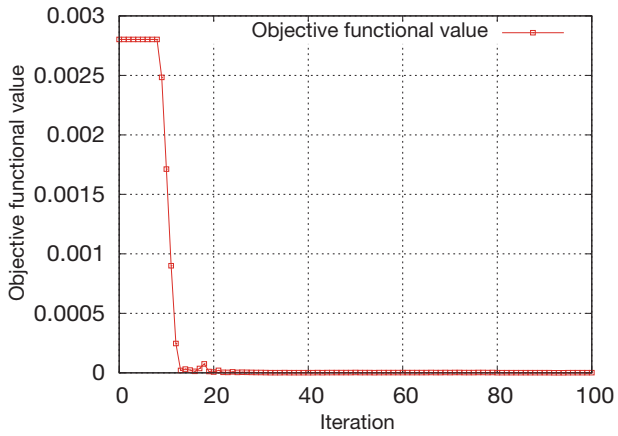

Fig. 9 Convergence curve of the objective functional J for the case of circular cavity.

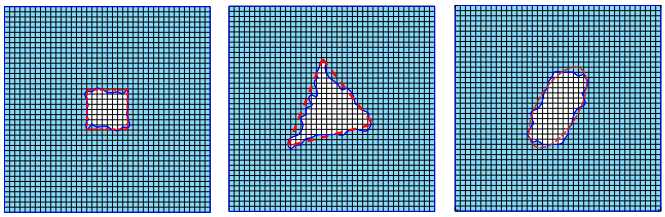

Fig. 10 The estimated shapes for the case of (left) square, (centre) triangle, and (right) oval cavities.

References

(1) Bendsøe, M.P., Kikuchi, N., Generating optimal topologies in structural design using a homogenization method, *Computer Methods in Applied Mechanics and Engineering*, Vol. 71, No. 2, pp. 197–224, 1988.

(2) Bendsøe, M.P., Optimal shape design as a material distribution problem, *Structural optimization*, Vol. 1, No. 4, pp. 193–202, 1989.

(3) Wang, M.Y., Wang, X., Guo, D., A level set method for structural topology optimization, *Computer methods in applied mechanics and engineering*, Vol. 192, No. 1, pp. 227–246, 2003.

(4) Allaire, G., Jouve, F., Toader, A.M., Structural optimization using sensitivity analysis and a level-set method, *Journal of computational physics*, Vol. 194, No. 1, pp. 363–393, 2004.

(5) Amstutz, S., Andrä, H., A new algorithm for topology optimization using a level-set method, *Journal of Computational Physics*, Vol. 216, No. 2, pp. 573–588, 2006.

(6) Yamada, T., Izui, K., Nishiwaki, S., Takezawa, A., A topology optimization method based on the level set method incorporating a fictitious interface energy, *Computer Methods in Applied Mechanics and Engineering*, Vol. 199, No. 45, pp. 2876–2891, 2010.

(7) Yang, R.J. Chen, C.J., Stress-based topology optimization, *Structural optimization*, Vol. 12, No. 2–3, pp. 98–105, 1996.

(8) Le, C., Norato, J., Bruns, T., Ha, C., Tortorelli, D., Stress-based topology optimization for continua, *Structural and Multidisciplinary Optimization*, Vol. 41, No. 4, pp. 605–620, 2010.

(9) Bruggi ,M., Duysinx, P., Topology optimization for minimum weight with compliance and stress constraints, *Structural and Multidisciplinary Optimization*, Vol. 46, No. 3, pp. 369–384, 2012.

(10) Delgado, G., Bonnet, M., The topological derivative of stress-based cost functionals in anisotropic elasticity, *Computers & Mathematics with Applications*, Vol. 69, No. 10, pp. 1144–1166, 2015.

(11) Isakari, H., Kuriyama, K., Harada, S., Yamada, T., Takahashi, T., Matsumoto, T., A topology optimisation for three-dimensional acoustics with the level set method and the fast multipole boundary element method, *Mechanical Engineering Journal*, Vol. 1, No. 4, pp. CM0039–CM0039, 2014.

(12) Guiggiani M., Casalini, P., Direct computation of cauchy principal value integrals in advanced boundary elements, *International Journal for Numerical Methods in Engineering*, Vol. 24, No. 9, pp. 1711–1720, 1987.